Journal of Hydrology (2007) 337, 207–223

available at www.sciencedirect.com

ScienceDirect

journal homepage: www.elsevier.com/locate/jhydrol

Seasonal, diurnal and storm-scale hydrochemical variations of typical epikarst springs in subtropical karst areas of SW China: Soil CO_2 and dilution effects

Zaihua Liu [a,b,c,*], Qiang Li [c], Hailong Sun [c], Jinliang Wang [c]

[a] *The State Key Laboratory of Environmental Geochemistry, Institute of Geochemistry, Chinese Academy of Science, 55002 Guiyang, China*
[b] *School of Resources and Environmental Sciences, Southwest University of China, 400715 Chongqing, China*
[c] *Karst Dynamics Laboratory, Ministry of Land and Resources, 50 Qixing Road, 541004 Guilin, China*

Received 14 April 2006; received in revised form 21 January 2007; accepted 23 January 2007

KEYWORDS
Hydrochemical variations;
Different time scales;
Epikarst springs;
Soil CO_2 effect;
Dilution effect;
Southwest China

Summary Two-year continuous pH, conductivity, temperature and water stage of the two typical epikarst springs, Nongla spring and Maolan spring (about 200 km apart) in subtropical karst areas of SW China were presented. Our primary study objective was to understand how karst systems respond hydrochemically to recharge at different time scales, and what the biogeochemical processes and controlling factors in the SW China epikarst environment are. A thermodynamic model was used to link the continuous data to monthly water quality data allowing the calculation of CO_2 partial pressures and calcite/dolomite saturation levels on a continuous basis. Marked seasonal, diurnal and storm-scale variations were observed for pH, conductivity, CO_2 partial pressures and calcite/dolomite saturation indexes of the springs, indicating that both springs are dynamic and variable systems. However, the coefficients of variation of these hydrogeochemical features tends to be in the order of seasonal $\geqslant$ storm-scale $>$ diurnal. The seasonal and diurnal variations of these features (higher conductivity and lower pH in summer and at daytime; lower conductivity and higher pH in winter and at nighttime) tend to co-vary with temperature which influences the production of CO_2 in soils, thus being the driving force for the variations (soil CO_2 effect). The storm-scale fluctuations occur during the spring-summer rainy days due to the storm-events. Depending on the rainfall intensities, however, there are differences in magnitudes and direction of the variations of these features. At very high rainfall intensity, the dilution effect dominates the variations, characterized by the decrease in both conductivity and calcite/dolomite saturation of the springs, while soil CO_2 effect determines the variations at lower rainfall intensity,

* Corresponding author. Address: Karst Dynamics Laboratory, Ministry of Land and Resources, 50 Qixing Road, 541004 Guilin, China. Tel.: +86 773 5837340; fax: +86 773 5837845.
E-mail addresses: zliu@karst.edu.cn, zaihua_liu@hotmail.com (Z. Liu).

0022-1694/$ - see front matter
doi:10.1016/j.jhydrol.2007.01.034

characterized by increase in CO_2 partial pressure and conductivity but decrease in pH and calcite/dolomite saturation. In a word, the hydrodynamic aspects together with hydrobiogeochemical characteristics need to be taken into account to correctly explain the hydrochemical variations of the epikarst springs. Results from the study demonstrate the need to redesign hydrogeochemical sampling strategies for epikarst springs in karst areas with monsoon climate like SW China (i.e., with remarkable seasonal matching fluctuations in temperature, rainfall and vegetation).

Introduction

Karst springs are important sampling points that are commonly used as monitoring locations to collect water-quality data at contaminated sites in karst hydrogeological regimes (Quinlan and Ewers, 1985). Abrupt changes in water quality in karst springs in response to rainfall events are well documented (Hess and White, 1988; Quinlan and Alexander, 1987; Ryan and Meiman, 1996). Quinlan and Alexander (1987) published guidelines for water-quality sampling frequency in karst terrains. Farmer and Williams (2001) showed that chloroform concentrations in a karst spring could vary as much as 60-fold throughout a storm cycle. Depending on the maturity of karst development and the nature of a rainfall event, each spring has a distinctive water-quality and discharge signature (Quinlan and Ewers, 1985). Despite these findings, little consideration has been given to the continuous behavior of water quality during a hydrological year, which includes seasonal, diurnal and storm-scale patterns in water quality. Quarterly and semi-annual samplings are still conducted at many contaminated karst sites.

In addition, information on variations in temperature, pH, $[HCO_3^-]$ and $[Ca^{2+}]$ in karst springs and their rivers is important in relation to:

(1) Determining partial pressure of CO_2 and calcite saturation within these waters (Neal et al., 2002; Liu et al., 2004);
(2) Assessing the balance between photosynthesis and respiration by biota and CO_2 transfers at the air—water interface (Maberly, 1996);
(3) Assessing the biological influences on CO_2 fluctuations in the water with respect to the precipitation/dissolution of calcite (Guasch et al., 1998; Liu et al., 2006);
(4) Understanding geochemical processes in karst aquifers and characterizing carbonate aquifers (Shuster and White, 1971; Andreo et al., 2002);
(5) Assessing karst-related carbon sink from atmosphere (Liu and Zhao, 2000).

Hydrochemographs of karst spring was used as indicators of aquifer characteristics by Raeisi and Karami (1997), and Andreo et al. (2002). However, hydrochemographs of con-

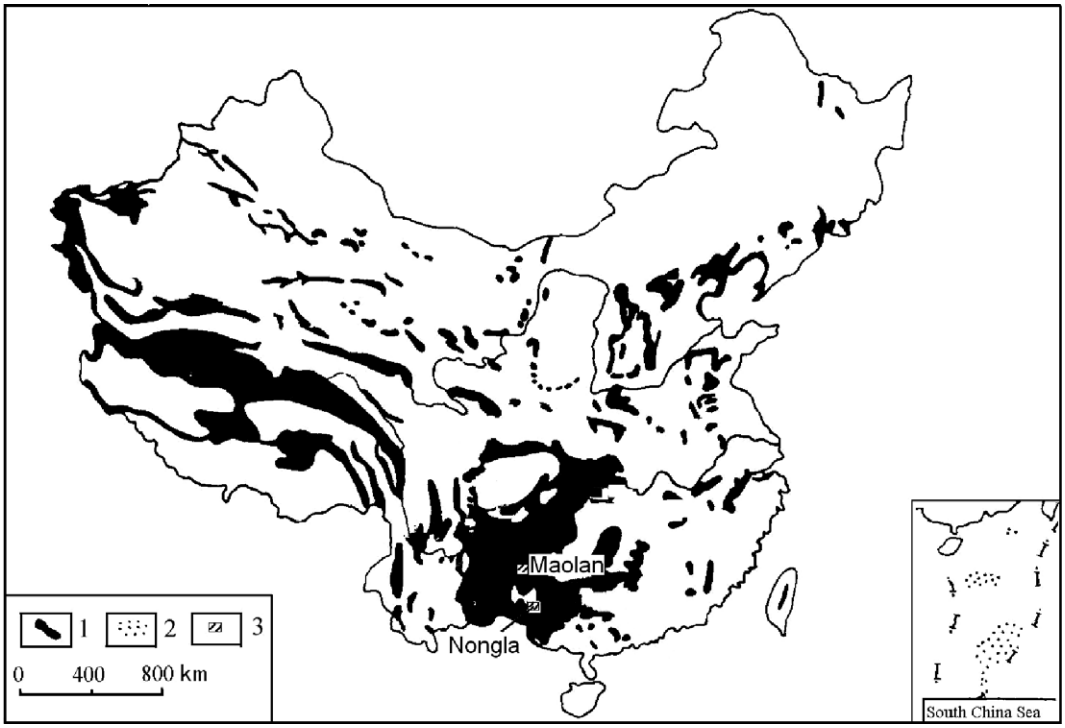

Figure 1 Distribution of carbonate rocks in China and the location of the two study sites, Nongla and Maolan. (1) carbonate rocks; (2) coral reef; and (3) study site.

tinuous water-quality data are needed to reveal these signatures.

Under the support of Ministry of Science and Technology of China and National Natural Science Foundation of China, we have been monitoring representative epikarst springs in karst areas of SW China since 2003 to evaluate the sensitivity of karst processes to environmental change induced by both nature and human being, and the suitability of the old hydrogeochemistry sampling strategies. The springs were continually monitored for temperature, water stage, pH and specific conductivity. This paper presents the two hydrological year continuous data from two of these springs, Nongla spring in Guangxi Province, and Maolan spring in Guizhou Province. It will be seen that marked seasonal, diurnal and storm-scale variations are found for pH, conductivity, CO_2 partial pressures and calcite/dolomite saturation of the springs. This shows the need to redesign hydrogeochemical sampling strategies for epikarst springs in subtropical karst areas of SW China. The results have important implications on how karst systems respond hydrochemically to recharge at different time scales, on the controlling factors on the carbon cycle in the epikarst zone, and to the understanding of water—rock interaction and hydrobiogeochemical processes in karst environment.

Study areas and their general settings

The two study areas, Nongla and Maolan Karst Experimental Sites, belong to subtropical karst areas of SW China. Their situations in China are shown in Fig. 1.

The Nongla Karst experimental site

Nongla in Guangxi province, SW China is famous for its typical epikarst (Field, 2002) development and quickly ecological restoration in 30 years after deforestation on fengcong karst (or peak cluster, Field, 2002). The lithology is mainly argillaceous and siliceous dolomite of the Donggangling Formation of middle Devonian. The annual mean temperature of Nongla is about 20 °C with hot summer and cold winter. The annual rainfall is 1756.6 mm, 80% of which falls in monsoonal rainy season of April to September. The thickness of soil is about 0—2 m, and the soil CO_2 content changes from 4500 ppmv to 35000 ppmv depending on the seasons and soil depth (Zhang et al., 2005). After 30 years of the ecological reconstruction, biodiversity increased remarkably, the habitation was improved and the community developed into a more stable stage. The local vegetation is mainly composed of natural forest (about 20%) and sparse secondary shrubs. A perennial epikarst spring (called Nongla spring) with flow rate of 0.01—20 l/s issues from the epikarst zone (~10 m in the recharge area to less than 0.1 m in discharge area) with conduit development (Photo 1). The spring issues from a water-filled conduit (diameter < 10 cm), and no tufa was present because of low calcite saturation index of the spring water (if $SIc \ll 1$, there will be no visible calcite deposition, Suarez, 1983; Dreybrodt, 1988). The catchment area of the spring could be larger than 0.05 km^2 determined according to topographic divide, because it is very common occurrence in karst areas that the topographic divide does not correspond to the groundwater divide.

Photo 1 The Nongla spring and its surrounding vegetation cover. The spring issues from a water-filled conduit, and no tufa was present because of low calcite saturation index of the spring water.

The Maolan Karst experimental site

Maolan in Guizhou Province, China is famous for its dense virgin evergreen forests growing on peak cluster karst. The Maolan Karst experimental site is situated in the northeast of Laqiao village, where a typical epikarst spring (called Maolan spring) issues with flow rate of 0.05—30 l/s (Photo 2). The spring issues from water-filled karst fractures, and no tufa was present because of low calcite saturation index of the spring water.

The catchment area of the spring could be larger than 0.06 km^2 determined according to topographic divide.

According to weather reports by local weather station (Zhou, 1987), annual rainfall at the site with virgin forest is about 1750 mm, ca 80% of which falls in monsoonal rainy season of April to September, while it is 400 mm lower in surrounding deforestation areas. The annual air temperature at the site is about 17 °C with hot summer (June—August) and cold winter (December—February). The rock in the site is mainly dolomitic limestone of Middle and Lower Carboniferous.

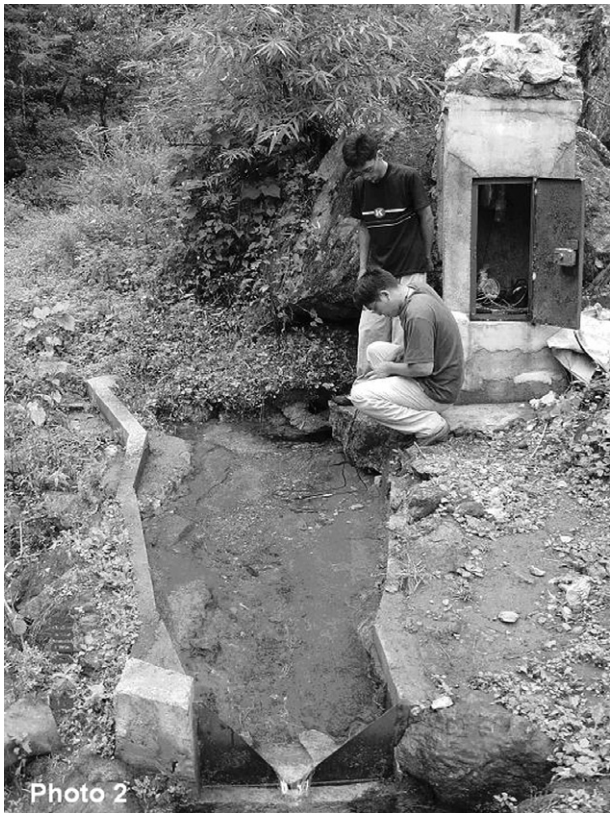

Photo 2 The Maolan spring and its surrounding vegetation cover. The spring issues from water-filled karst fractures, and no tufa was present because of low calcite saturation index of the spring water.

Methods

Automatic monitoring of rainfall, water stage, water temperature, pH and specific conductivity

To measure detailed hydrochemical variations in the conduit and diffuse flow conditions (Shuster and White, 1971; Atkinson, 1977), a Greenspan CTDP 300 multi-channel data logger (Liu et al., 2004) was used in Nongla spring and Maolan spring respectively, which include the diffuse flow from karst fracture and/or conduit flow from karst conduits (the sensors being fixed tightly in a PVC tube with small holes on its wall, and then the PVC tube was located in flowing spring water about 10 cm below base flow's surface). Rainfall, water stage, water temperature, pH and specific conductivity have been monitored every 15 min since March of 2003. The logger was calibrated prior to deployment using pH (4, 7 and 10) and conductivity (1412 μs/cm) standards. Hand-held water quality meter (WTW MultiLine P3 pH/LF-SET) measurements were undertaken to check the reliability of data logger measurements at monthly interval, when retrieving data from data logger was conducted in each month. It was found that hand held meter and logger measurements are identical within 3% error.

Analysis of concentrations of major ions in rain water and springs

In situ titrating was used to measure the $[HCO_3^-]$ and $[Ca^{2+}]$ of water with the Aquamerck Alkalinity Test and Hardness Test monthly. The resolutions are 6 and 1 mg/l, respectively.

To understand the general chemistry of other major ions in the systems, water samples from the two springs were collected by filtering with 0.45 μm Minisart® filter and analyzed in the laboratory at a monthly interval for two-years. For comparison, some samples of rainwater were also analyzed. The analysis methods used were standard titration for bicarbonate, atomic absorption for K^+ and Na^+, titration with EDTA for Ca^{2+}, Mg^{2+} and SO_4^{2-}, and the Mohr titration for Cl^-.

Results

Estimating CO_2 partial pressure and calcite/dolomite saturation index from continuous records of temperature, pH and specific conductivity

The CO_2 partial pressure and calcite/dolomite saturation index of spring water are related to its calcium, magnesium and bicarbonate concentrations, pH and temperature as described in an earlier study (Liu et al., 2004). However, while the continuous monitors directly measure pH and temperature, continuous calcium, magnesium and bicarbonate concentrations have to be estimated indirectly. In the case of the two study sites, the spring composition is dominated by calcite/dolomite dissolution. So, calcium and magnesium are the major cations and bicarbonate is the major counterbalancing anion. Consequently, these ions dominate the electrical conductivity and their concentrations are directly proportional to the electrical conductivity. As the electrical conductivity is directly measured continuously, this feature is used to estimate calcium, magnesium and bicarbonate concentrations from the continuous electrical conductivity data. For this purpose, the linkages between concentrations and electrical conductivity need to be established from the spot-sampled monthly data.

At the Nongla experimental site, these concentrations are linearly related to specific conductivity by the relationships

$$[Ca^{2+}] = 0.133spc - 0.01, \quad r^2 = 0.9997, \tag{1}$$

$$[Mg^{2+}] = 0.0654spc, \quad r^2 = 0.999, \tag{2}$$

$$[HCO_3^-] = 0.699spc - 5.36, \quad r^2 = 0.998 \tag{3}$$

and for the Maolan experimental site, the relationships are:

$$[Ca^{2+}] = 0.15spc - 0.78, \quad r^2 = 0.94, \tag{4}$$

$$[Mg^{2+}] = 0.04spc + 0.22, \quad r^2 = 0.77, \tag{5}$$

$$[HCO_3^-] = 0.63spc - 4.70, \quad r^2 = 0.99, \tag{6}$$

where brackets denote species concentrations in mg/L and spc is specific conductivity in μS/cm at 25 °C.

This information is used with the electrical conductivity data to determine continuous changes in carbon dioxide and calcite/dolomite saturation levels.

The full hydrochemical data sets, including recorded temperature and pH, calculated Ca^{2+}, Mg^{2+} and HCO_3^- through the regression equation above, mean monthly values of K^+, Na^+, Cl^- and SO_4^{2-} (Table 1), were processed through the program WATSPEC (Wigley, 1977), which calculates CO_2 partial pressure (P_{CO_2}) and saturation indexes of calcite ($SI_{calcite}$) and dolomite ($SI_{dolomite}$) for each record. P_{CO_2} assumed to be in equilibrium with the sampled waters is calculated from:

$$P_{CO_2} = \frac{(HCO_3^-)(H^+)}{K_H K_1}, \tag{7}$$

where parenthesis denotes species activity in mol/L, and K_H and K_1 are the temperature-dependent Henry's Law and first dissociation constants for CO_2 gas in water, respectively.

$SI_{calcite}$ and $SI_{dolomite}$ are calculated from:

$$SI_{calcite} = \log\left(\frac{(Ca^{2+})(CO_3^{2-})}{K_{calcite}}\right), \quad \text{and}$$

$$SI_{dolomite} = \log\left(\frac{(Ca^{2+})(Mg^{2+})(CO_3^{2-})^2}{K_{dolomite}}\right) \tag{8}$$

respectively, where $K_{calcite}$ and $K_{dolomite}$ are the temperature-dependent equilibrium constant for calcite and dolomite respectively (Drever, 1988; Stumm and Morgan, 1981). If SI > 0, water is supersaturated with respect to the mineral; if SI < 0, water is aggressive to the mineral; and if SI = 0, the equilibrium reaches.

Results

The results of this work are extensive and summarizing the findings is difficult without reference to the full dataset. Statistical analysis (Tables 1–3) simply does not convey the detail of the record and the data is therefore presented graphically in time series to allow visual assessment alongside the summary text. The time series comprises three levels of detail. Firstly, time series for the full data record are presented in Figs. 2 and 3 for Nongla spring and Maolan spring, respectively. The two figures show the seasonal variability superimposed on the fine detail of diurnal

Table 1 The general chemistry of major ions in the rain water and springs at the two study sites

Site	Water temperature (°C)	pH	K^+ (mg/l)	Na^+ (mg/l)	Ca^{2+} (mg/l)	Mg^{2+} (mg/l)	Cl^- (mg/l)	SO_4^{2-} (mg/l)	HCO_3^- (mg/l)	spc. (μs/cm 25 °C)	$SI_{calcite}$	$SI_{dolomite}$	P_{CO_2} (ppmv)	N
NL–SW–CD	14.8	7.35	0.20	0.35	64.93	31.93	4.05	5.16	335.92	488	0.06	−0.01	13345	16
NL–SW–WW	19.6	7.33	0.22	0.28	71.46	35.14	5.06	6.14	370.25	537	0.18	0.30	16111	17
NL–RW–WW	19.0	7.23	0.25	0.02	2.45	1.00	1.86	0.00	9.17	12	−2.80	−5.75	523	4
ML–SW–CD	16.4	7.66	0.13	0.23	45.60	12.60	2.03	11.08	190.22	309	0.04	−0.20	4853	16
ML–SW–WW	17.0	7.38	0.17	0.25	46.90	12.94	2.03	11.29	195.57	318	−0.21	−0.72	7625	17
ML–RW–WW	17.0	7.17	0.10	0.06	2.28	0.48	1.77	0.00	6.66	10	−3.05	−6.58	427	4

NL, ML: abbreviations for Nongla and Maolan, respectively; SW, RW for spring water and rain water, respectively; CD, WW for cold dry season and warm wet season; N: number of samples.

Table 2 Statistics on the seasonal and diurnal variations of physicochemical parameters of the two epikarst springs

Spring name	Nongla		Maolan	
Time scale	Seasonal	Diurnal	Seasonal	Diurnal
Water temperature (°C)	7.6—21.98[a](17.58)[b][18.8][c]	19.19—20.28[a](19.72)[b][1.6][c]	13.82—18.91 (16.53)[6.7]	17.70—17.76 (17.73)[0.1]
Spc (μs/cm, 25 °C)	182—633 (534)[13.3]	616—632 (624)[0.7]	213—391 (310)[5.9]	309—316 (312)[0.5]
pH	6.96—8.05 (7.41)[2.3]	7.31—7.43 (7.38)[0.4]	7.06—8.09 (7.57)[3.3]	7.52—7.76 (7.66)[1]
$SI_{calcite}$	−0.50—0.90 (0.24)	0.30—0.41 (0.36)	−0.60—0.43 (−0.04)	−0.06—0.17 (0.07)
$SI_{dolomite}$	−1.05—1.74 (0.38)	0.55—0.77 (0.67)	−1.54—0.49 (−0.4)	−0.47—−0.01 (−0.20)
P_{CO_2} (ppmv)	2355—38,370 (13,414)[40]	14,060—18,967 (16,046)[8]	1262—15,740 (5439)[62]	2965—5212 (3801)[18]

[a] Minimum—maximum.
[b] Mean values (N = 70,080).
[c] C.v. or coefficient of variation = (standard deviation/mean)%, c.v.s are not reported for $SI_{calcite}$ and $SI_{dolomite}$ values as these can be positive or negative.

Table 3 Statistics on the storm-scale variations of physicochemical parameters of the two epikarst spring

Spring name	Nonlgla		Maolan	
Storm name	May storm in 2003 (136 mm/7 h)	May storm in 2004 (120 mm/6 h)	July 3 storms in 2003 (177.5 mm/18 h)	July 3 storms in 2004 (101 mm/10 h)
Water temp.(°C)	19.49—21.50[a](19.65)[b] [1.4][c]	19.09—20.01 (19.31) [1.2]	17.01—18.29[a](17.56)[b] [1.8][c]	17.15—18.02 (17.53)[1.2]
Spc (μs/cm, 25 °C)	182—600 (531)[14]	250—493 (411)[15]	238—346 (310)[6.1]	300—344 (319)[3.1]
pH	7.21—7.48 (7.26)[0.8]	7.14—7.44 (7.29)[1.1]	7.20—7.53 (7.42)[1.8]	7.38—7.55 (7.51)[0.5]
$SI_{calcite}$	−0.50—0.30 (0.11)	−0.47—0.23 (−0.08)	−0.60—−0.08 (−0.17)	−0.20—−0.02 (−0.06)
$SI_{dolomite}$	−1.05—0.54 (0.15)	−1.00—0.39 (−0.23)	−1.54—−0.50 (−0.67)	−0.74—− 0.39 (−0.46)
P_{CO_2} (ppmv)	3837—22,080 (18,251)[21]	7907—17,906 (13,145)[17.8]	4864—10,116 (6610)[25]	4764—7638 (5468)[11.6]

[a] Minimum—maximum.
[b] Mean values (N = 70,080).
[c] C.v. or coefficient of variation = (standard deviation/mean)%, c.v.s are not reported for $SI_{calcite}$ and $SI_{dolomite}$ values as these can be positive or negative.

and storm-scale fluctuations. Secondly, a more detailed time series showing diurnal fluctuations for the two springs are presented in Figs. 4 and 5 for a two-day time series from November 1, 2003 through November 3, 2003. These two figures provide a graphical representation of the regularity and variability within the diurnal fluctuations. Thirdly, time series patterns are presented in Figs. 6a and 6b for Nongla spring for Storm-scale variations on May 24, 2003 and May 16, 2004, respectively, and in Figs. 7a and 7b for Maolan spring for Storm-scale variations on July 6—7, 2003 and July 19—20, 2004, respectively to show dilution and soil CO_2 effects under different rainfall intensity.

The most noticeable points to the time series are as follows.

Water temperature

The water temperature patterns show similar features for both sites (Figs. 2 and 3). However, at Nongla site, the temperatures are three degree higher during the summer and about one degree lower during the winter than for the Maolan site, and thus show larger variability (c.v. = 18.8% for Nongla spring, and 6.7% for Maolan spring, Table 2). Temperature shows both seasonal and daily patterns of change. The seasonal pattern (Figs. 2 and 3) is represented by a yearly cycle of change while the daily patterns (Figs. 4 and 5) are represented by diurnal oscillations but weaker for Maolan spring (Table 2). In addition, during hot summer months, spring water temperatures typically increase after rainfall, and show synchronous variation with water stage (Figs. 6a, 6b, 7a and 7b). It seems that the larger the water stage change, the higher the water temperature (Figs. 6a vs. 6b, Figs. 7a vs. 7b).

Electrical conductivity

Electrical conductivity shows similar features for both sites in seasonal pattern (Figs. 2 and 3). However, at Maolan site, the electrical conductivity is ca 200 μS/cm lower on the average with low variability (c.v. = 5.9% for Maolan spring, and 13.3% for Nongla spring, Table 2). Electrical conductiv-

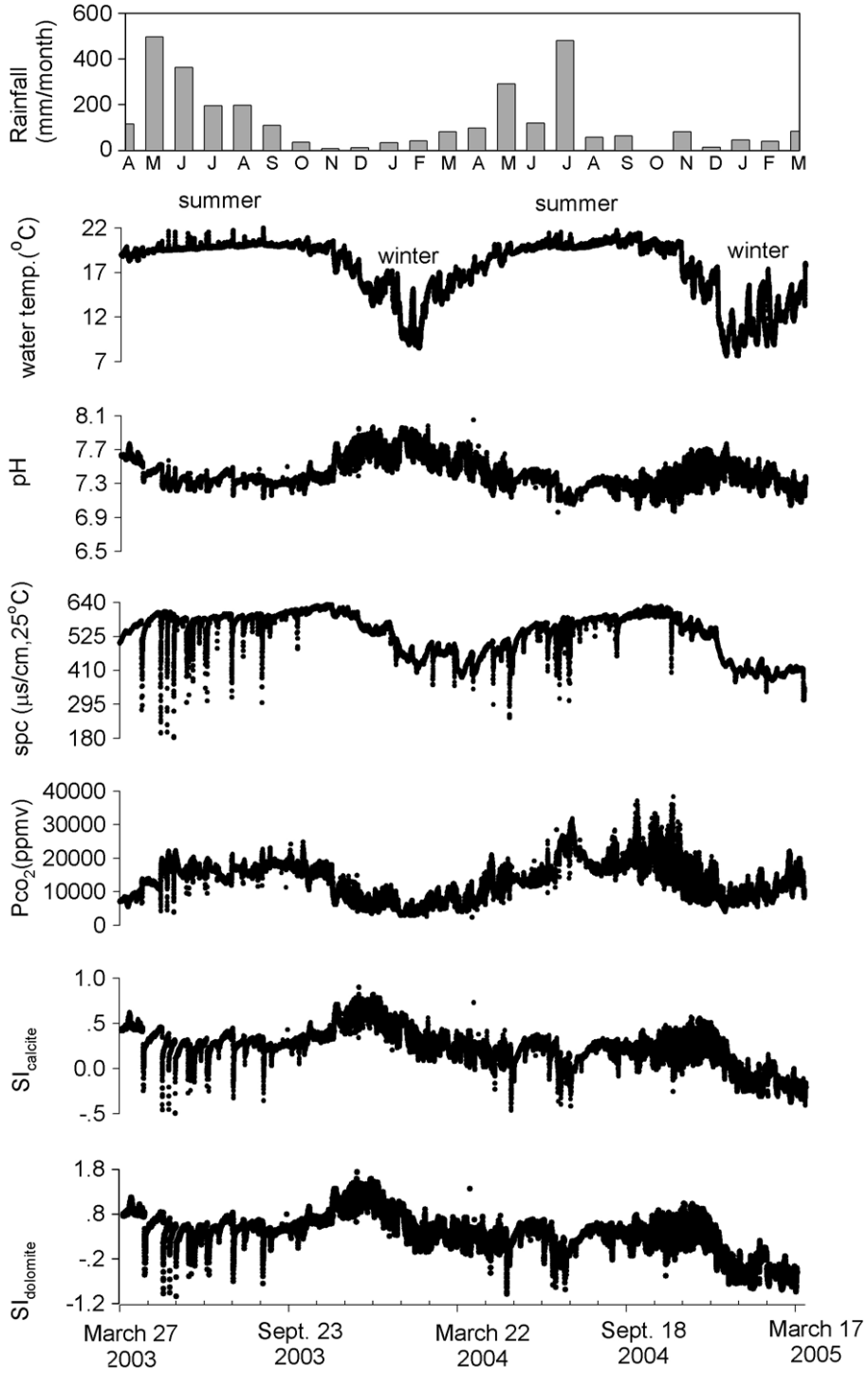

Figure 2 Continuous data of water temperature, pH, specific conductivity (spc), calculated CO_2 partial pressure (P_{CO_2}), calcite saturation index ($SI_{calcite}$) and dolomite saturation index ($SI_{dolomite}$) from Nongla epikarst spring at 15-min intervals, March 27, 2003 through March 27, 2005. Marked seasonal cycles are found, where P_{CO_2} and spc show in-phase change with temperature, while pH, $SI_{calcite}$ and $SI_{dolomite}$ show inverse change with temperature.
Note: For the spring water stage, the value has only qualitative meaning due to the excursion of water level caused by the sensor. Considering this, the seasonal flow has not been shown in the figure.

ity shows both seasonal and daily patterns of change. The seasonal pattern (Figs. 2 and 3) is represented by a yearly cycle of change (higher in summer and lower in winter) while the daily variations (Figs. 4 and 5) are characterized by higher value at daytime and lower value at nighttime. In addition, electrical conductivity typically decreases after rainfall, and shows reverse variation with water stage (Figs. 6a, 6b and 7a). However, for Maolan spring, electrical con-

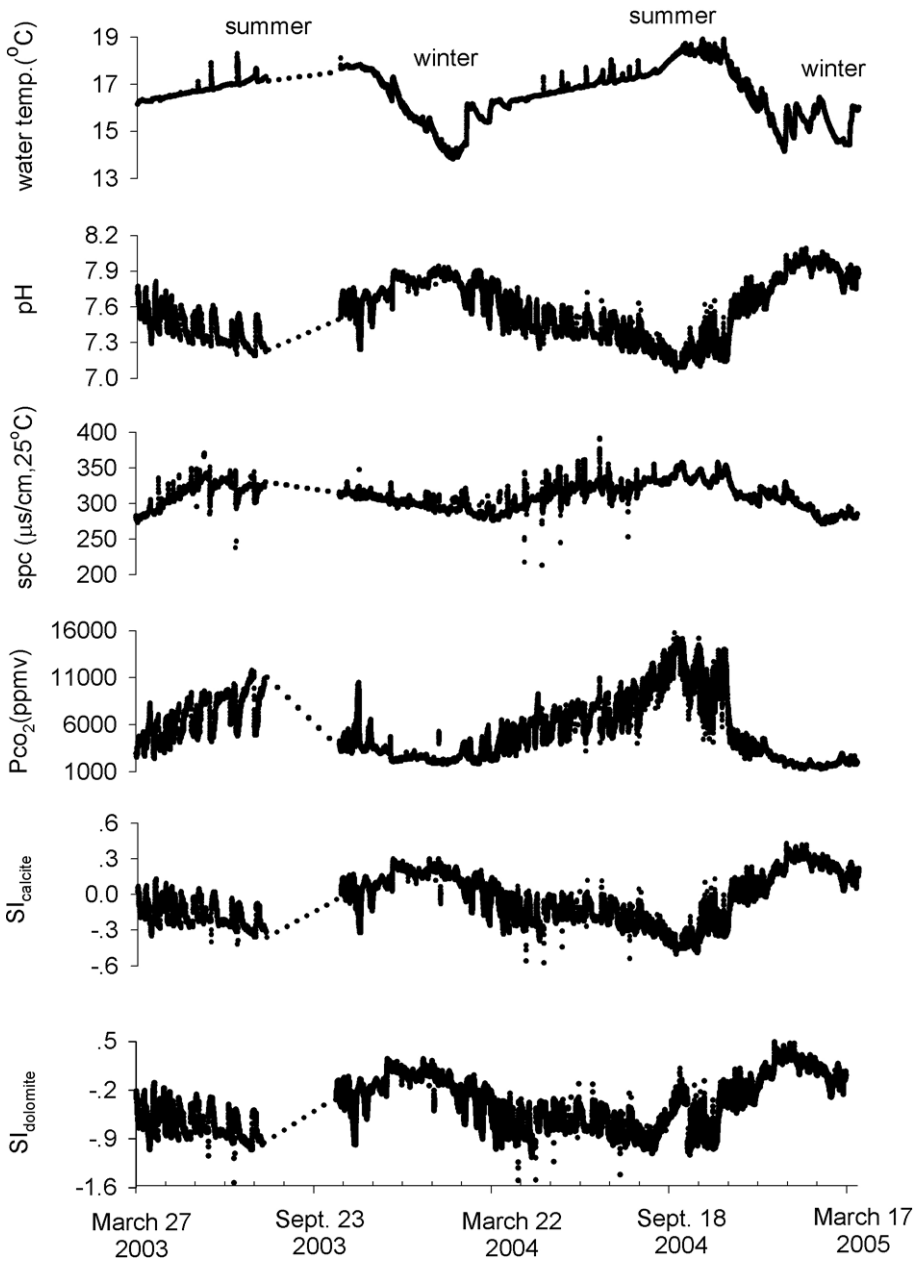

Figure 3 Continuous data of water temperature, pH, specific conductivity (spc), calculated CO_2 partial pressure (P_{CO_2}), calcite saturation index ($SI_{calcite}$) and dolomite saturation index ($SI_{dolomite}$) from Maolan epikarst spring at 15-min intervals, March 27, 2003 through March 27, 2005. (dotted line: no data due to the repairing of the dada logger). Marked seasonal cycles are found, where P_{CO_2} and spc show in-phase change with temperature, while pH, $SI_{calcite}$ and $SI_{dolomite}$ show inverse change with temperature.
Note: There were some errors in rainfall records of Maolan site due to road construction. For the spring water stage, the value has only qualitative meaning due to the excursion of water level caused by the sensor. Considering these, the seasonal flow and rainfall data have not been shown in the figure.

ductivity increases after rainfall when rainfall intensity becomes lower (Fig. 7b).

pH

pH shows both a seasonal and a diurnal pattern (Figs. 2—5). Overall, the waters have a pH in the range 6.96—8.09, lower in the summer and higher in the winter. During dry weather in the autumn, the diurnal changes (lower at daytime and higher at nighttime) can be 0.1—0.2 units. pH generally decreases after rainfall, and show reverse variation with water stage (Figs. 6b, 7a and 7b). However, in some cases, pH increases after rainfall (Fig. 6a).

CO_2 partial pressure

P_{CO_2} show similar features for both sites in seasonal pattern (Figs. 2 and 3). However, at Maolan site, the P_{CO_2} is

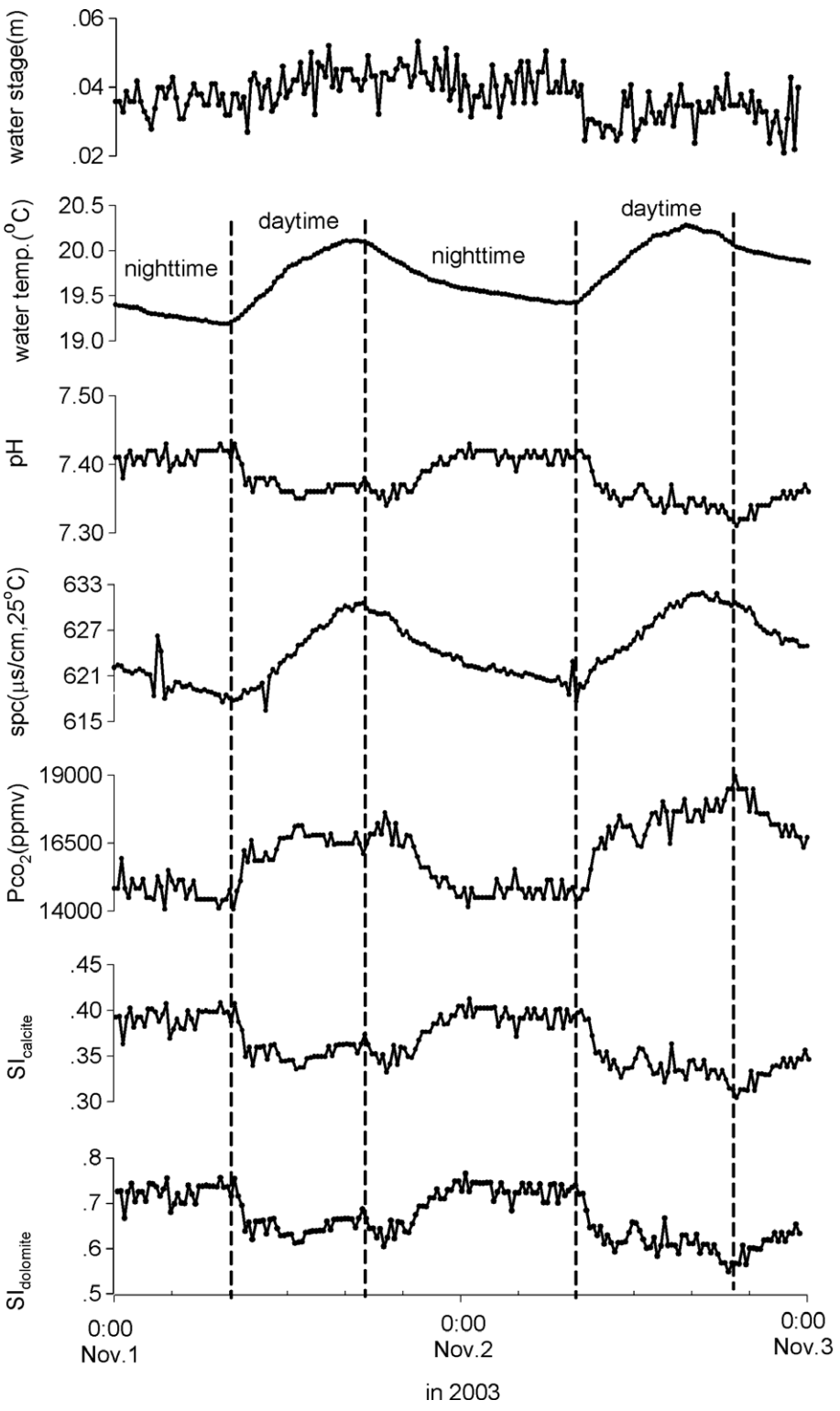

Figure 4 A two-day time series for water temperature, pH, specific conductivity (spc), calculated CO_2partial pressure (P_{CO_2}), calcite saturation index ($SI_{calcite}$) and dolomite saturation index ($SI_{dolomite}$) from Nongla epikarst spring at 15-min intervals, November 1, 2003 through November 2, 2003. Marked diurnal cycles are found, where P_{CO_2} and spc show in-phase change with temperature, while pH, $SI_{calcite}$ and $SI_{dolomite}$ show inverse change with temperature.

ca 8000 ppmv lower on the average with high variability (62% for Maolan spring, and 40% for Nongla spring, Table 2). P_{CO_2} change shows both seasonal and daily patterns. The seasonal pattern (Figs. 2 and 3) is represented by a yearly cycle (higher in summer and lower in winter) while the daily variations (Figs. 4 and 5) are characterized by

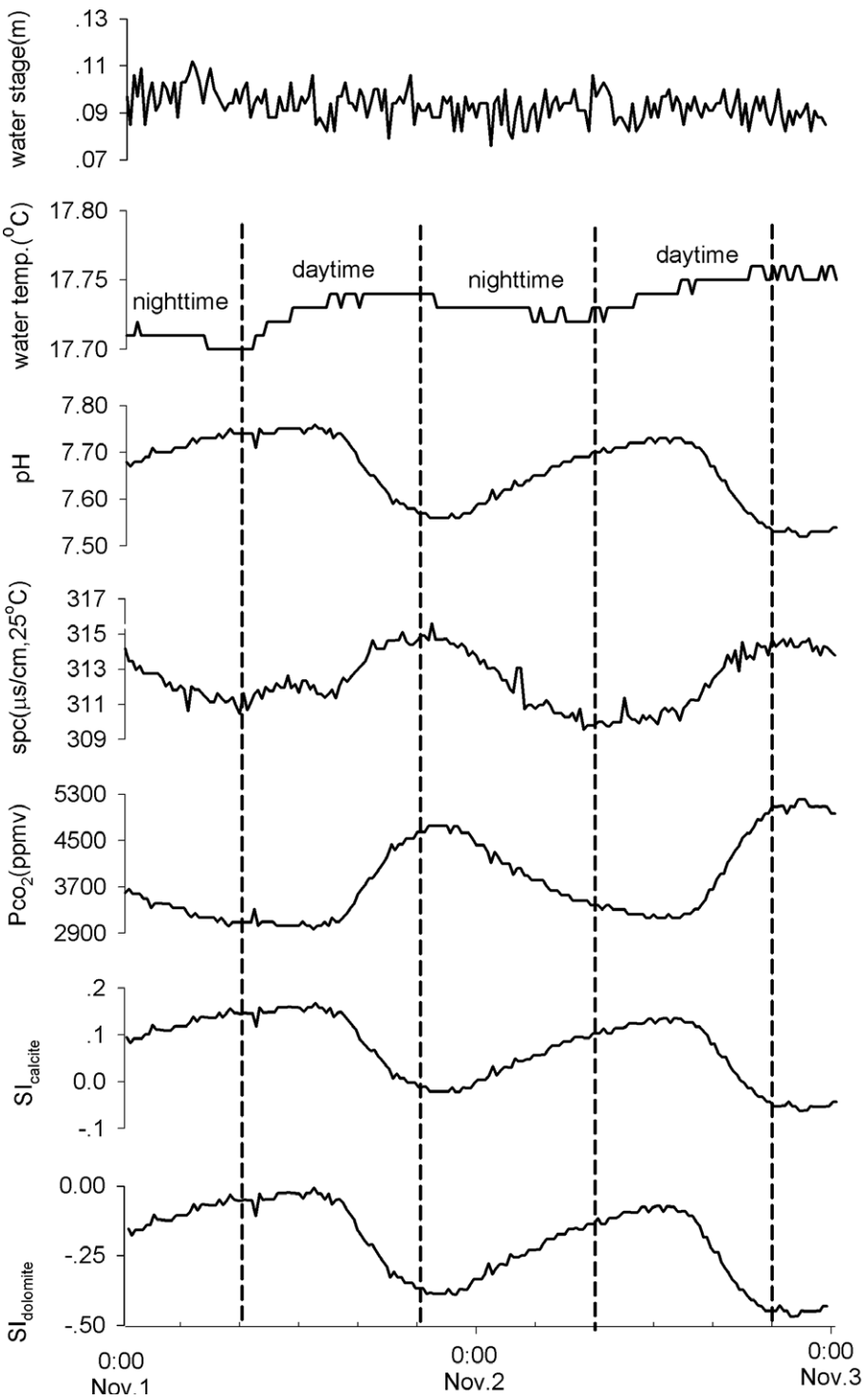

Figure 5 A two-day time series for water temperature, pH, specific conductivity (spc), calculated CO_2partial pressure (P_{CO_2}), calcite saturation index ($SI_{calcite}$) and dolomite saturation index ($SI_{dolomite}$) from Maolan epikarst spring at 15-min intervals, November 1, 2003 through November 2, 2003. Similar marked diurnal cycles to Nongla spring are also found.

higher value at daytime and lower value at nighttime. In addition, P_{CO_2} generally decreases after heavy rainfall, and show reverse variation with water stage (Figs. 6a, 6b and 7a). However, for Maolan spring, P_{CO_2} increases after rainfall when rainfall intensity becomes lower (Fig. 7b, Table 3).

Calcite and dolomite saturation indexes

The water is mainly oversaturated with respect to calcite and dolomite for Nongla spring across the whole period of record except during storm events (Fig. 2) while it is undersaturated for Maolan spring except in winter (Fig. 3). The

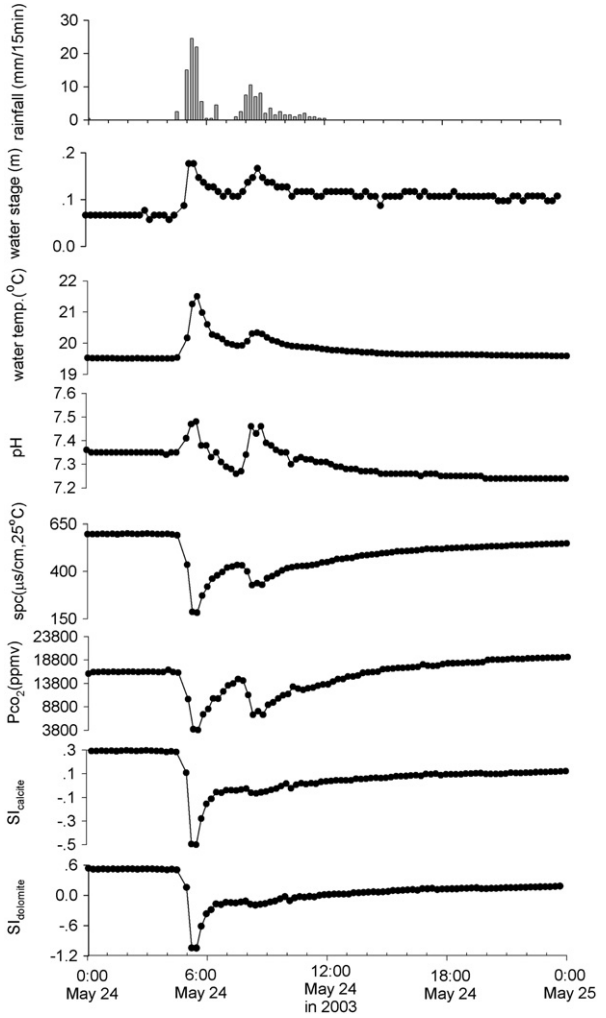

Figure 6a Storm-scale variations in water temperature, pH, specific conductivity (spc), calculated CO_2 partial pressure (P_{CO_2}), calcite saturation index ($SI_{calcite}$) and dolomite saturation index ($SI_{dolomite}$) from Nongla epikarst spring at 15-min intervals, May 24, 2003. Dilution effects are found, where spc, P_{CO_2}, $SI_{calcite}$ and $SI_{dolomite}$ decrease when storms come.

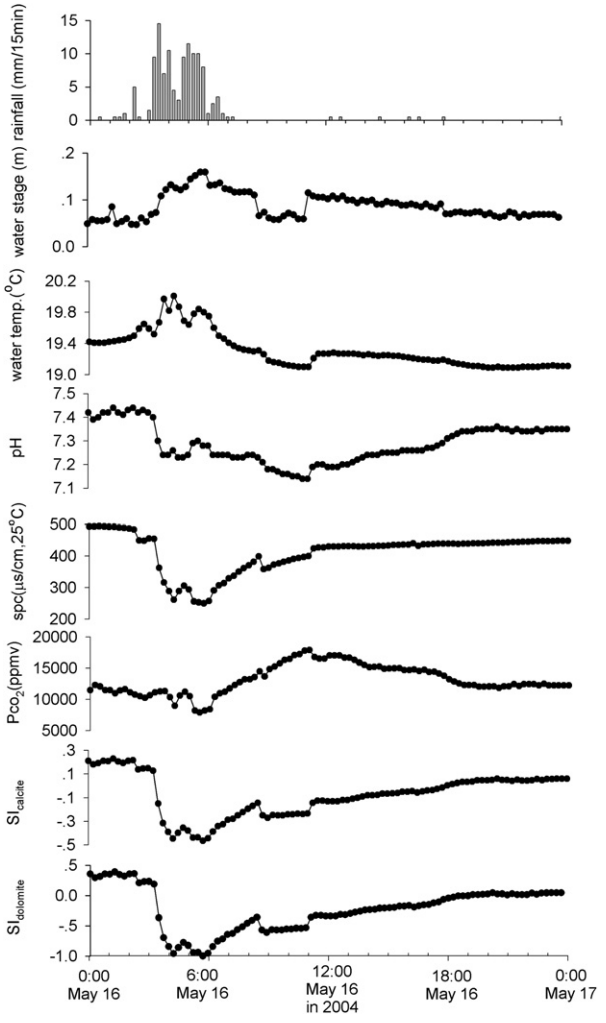

Figure 6b Storm-scale variations in water temperature, pH, specific conductivity (spc), calculated CO_2 partial pressure (P_{CO_2}), calcite saturation index ($SI_{calcite}$) and dolomite saturation index ($SI_{dolomite}$) from Nongla epikarst spring at 15-min intervals, May 16,2004. Dilution effects are found, where spc, $SI_{calcite}$ and $SI_{dolomite}$ decrease when storms come.

degree of oversaturation increases in winter times and decreases in the summer times. Furthermore, a marked diurnal pattern (lower at daytime and higher at nighttime) is observed (Figs. 4 and 5). In addition, calcite and dolomite saturation indexes decrease after rainfall in all cases, and show reverse variation with water stage (Figs. 6a, 6b and 7a, 7b).

Discussions

The results described provide a major source of hydrochemical data for the two sites. Within this discussion section there are three main components: (1) temporal patterns for the two sites; (2) comparison of hydrochemistry between the two sites, and (3) comparison with spring sites elsewhere in the world. These three aspects are considered separately below, before the information is brought together in section ''Conclusions''.

Temporal hydrochemical variations of the Nongla and Maolan springs

The time series exhibits three types of variation patterns in temperature, pH, electrical conductivity, P_{CO_2} and calcite/dolomite saturation: a cyclical seasonal pattern, a cyclical diurnal pattern and storm-scale fluctuation. These aspects are considered separately below in relation to the different determinants.

Temperature

The temperature fluctuations represent normal behavior for SW China epikarst springs and are comprised of three components. Firstly, the annual cyclic variation in air temperature leads to a sinusoidal pattern in the spring temperature (Fig. 8): maxima during the summer months and minima during the winter months. Secondly, there is a diurnal pattern observed which relates to the absorption of solar radi-

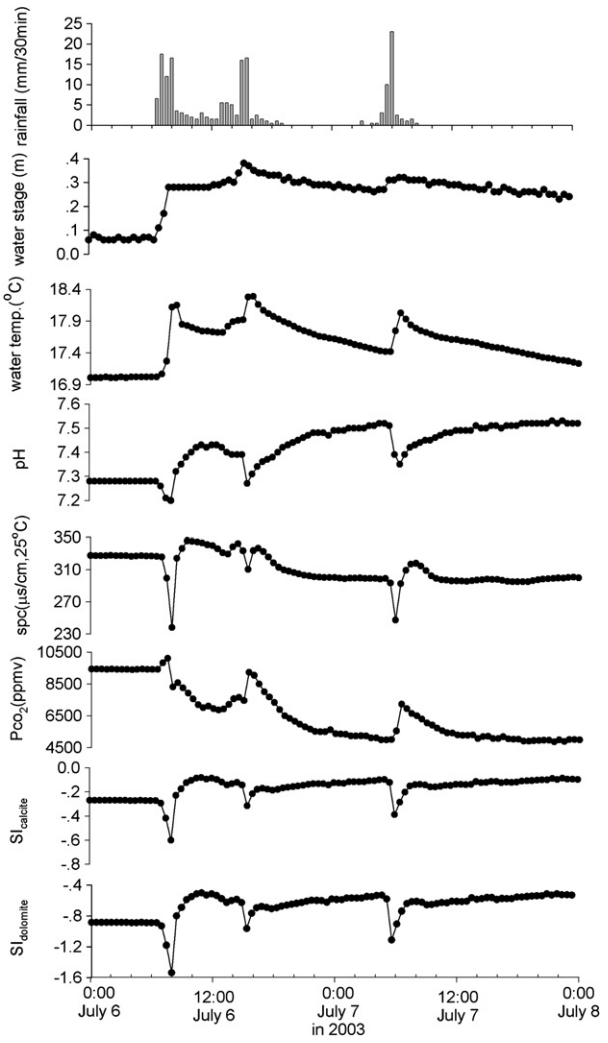

Figure 7a Storm-scale variations in water temperature, pH, specific conductivity (spc), calculated CO_2 partial pressure (P_{CO_2}), calcite saturation index ($SI_{calcite}$) and dolomite saturation index ($SI_{dolomite}$) from Maolan epikarst spring at 15-min intervals, July 6—7, 2003. Dilution effects are found, where spc, $SI_{calcite}$ and $SI_{dolomite}$ decrease when storms come.

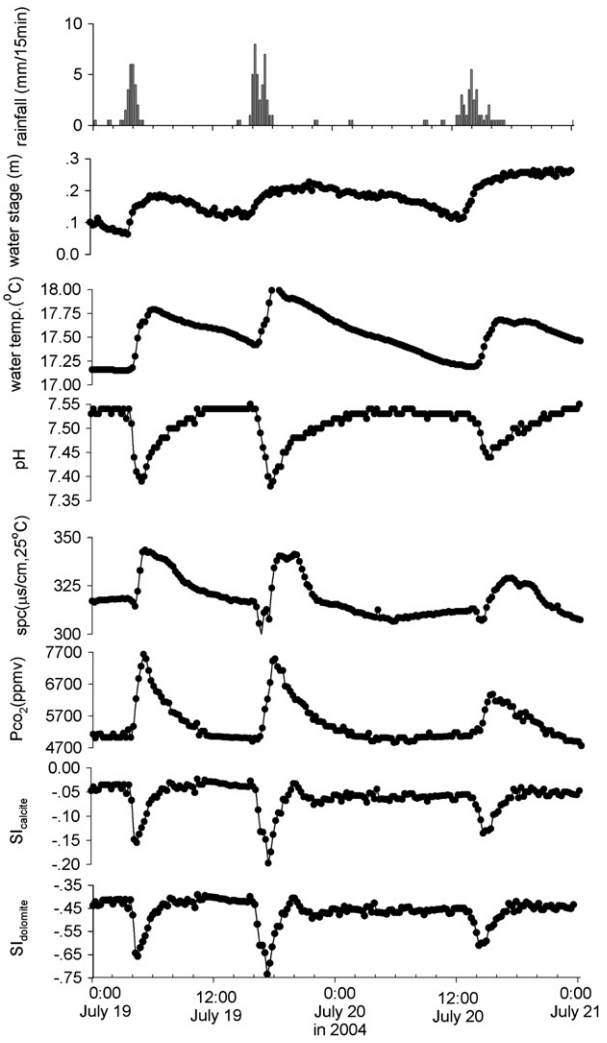

Figure 7b Storm-scale variations in water temperature, pH, specific conductivity (spc), calculated CO_2 partial pressure (P_{CO_2}), calcite saturation index ($SI_{calcite}$) and dolomite saturation index ($SI_{dolomite}$) from Maolan epikarst spring at 15-min intervals, July 19—20, 2004. Soil CO_2 effects are found, where P_{CO_2} and spc increase, while pH, $SI_{calcite}$ and $SI_{dolomite}$ decrease when storms come if dilution effects are not strong enough.

ation by the shallow epikarst zones, which feed the springs. For this, the solar absorption is maximal during the day. Of course, the solar radiation into the surface water of the spring may also have influence on diurnal variations of water temperature. However, this is small, considering the temperature sensors were located in the flowing spring waters but not in pools. Thirdly, during hot summer months, solar radiation heats rainwater, so spring water temperatures typically increase after rainfall, and show synchronous variation with water stage (Figs. 6a, 6b and 7a, 7b).

CO_2 partial pressure

The CO_2 partial pressure in water (P_{CO_2}) is strongly related to the respiration by plant roots and microbe in the soils. In general, in summer and during the day root respiration in soil is stronger and hence carbon dioxide is more generated (Atkin et al., 2000). This is the reason why the seasonal pattern in P_{CO_2} (Figs. 2 and 3) is shown by a yearly cycle of change (higher in summer and lower in winter) while the daily patterns (Figs. 4 and 5) are shown by higher value at daytime and lower value at nighttime. The decrease in P_{CO_2} after rainfall for Nongla spring (Figs. 6a, 6b) and heavy rainfall for Maolan spring (Fig. 7a) is due to the dilution effect by rain water via karst conduit and/or overland flow, and shows reverse variation with water stage. However, for Maolan spring, the increase in P_{CO_2} after low rainfall (Fig. 7b) is mainly related to the dissolving of soil CO_2 (with higher partial pressure in summer) into infiltrating rainwater, which feeds the epikarst spring (soil CO_2 effect, Liu et al., 2004).

Electrical conductivity

Electrical conductivity is a measure of the number of ions in solution. For the two study sites, these ions are mainly calcium, magnesium and bicarbonate. The seasonal pattern in

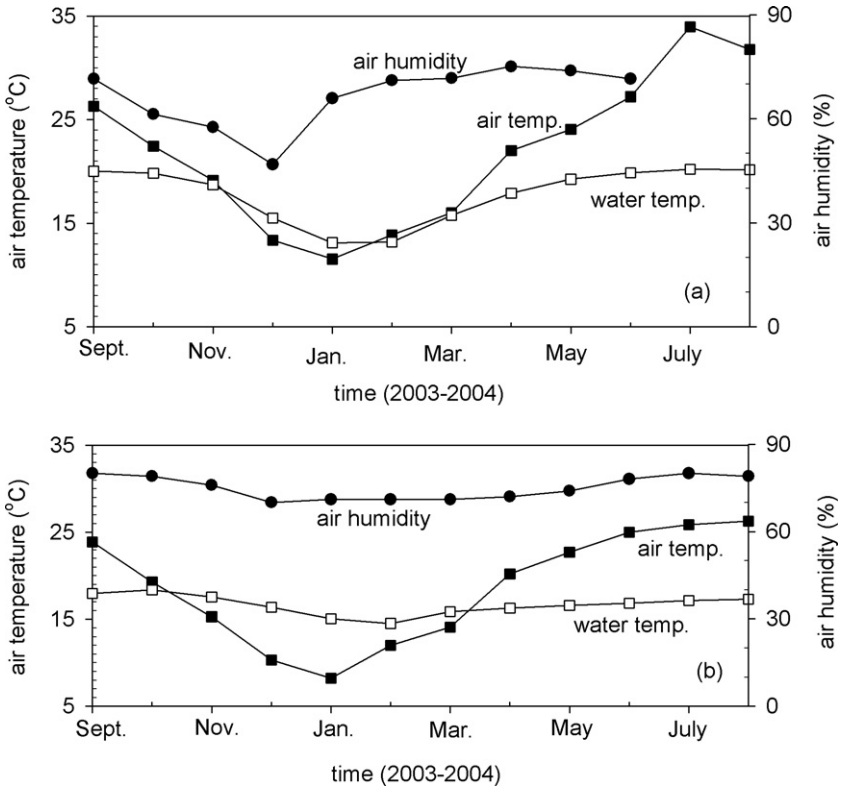

Figure 8 Monthly air temperature, humidity and spring water temperature at Nongla (a) and Maolan (b) sites.

electrical conductivity at both sites (Figs. 2 and 3) is related to the seasonal variation in soil CO_2, which dissolves into water, and increases the dissolution of limestone and dolomite (Liu et al., 1998; Liu and Zhao, 2000). The daily patterns in electrical conductivity (Figs. 4 and 5) may be determined by diurnal oscillations in root respiration (higher at daytime and lower at nighttime, Atkin et al., 2000; Liu et al., 2006), which contribute to the variation in water P_{CO_2}, and thus the dissolution or precipitation of carbonate. The decrease in electrical conductivity after heavy rainfall is related to the dilution effect by rain water via karst conduit and/or overland flow, and shows reverse variation with water stage (Figs. 6a, 6b and 7a). However, for Maolan spring, the increase in electrical conductivity after lower rainfall (implying weak dilution effect) (Fig. 7b) is mainly controlled by the soil CO_2 effect (Liu et al., 2004), because less soil CO_2 could release to the atmosphere, but more soil CO_2 dissolves into water at this time, which decreases the pH of water, and thus increases the dissolution of carbonate rocks in the epikarst aquifer. If the increase in electrical conductivity is due to longer residence time in the aquifer, the water should have higher pH, higher calcite saturation index, and lower P_{CO_2}, which is just opposite to the real case we observed. So, the shunting out of groundwater with longer residence time can only explain the higher electrical conductivity but not the higher P_{CO_2}, lower pH and lower calcite saturation index.

On the other hand, the concentration resulting from increased evaporation in summer has to be taken into account, even though it is likely to be small because of the high humidity (Fig. 8) accompanying the monsoonal summer rainfall. The ratio of average summer concentration to average winter concentration for almost all species in Nongla spring is ~1.1, including species that are likely to represent input entirely through rainfall, like Cl^- and SO_4^{2-} (Table 1). This implies strongly that evaporation is influencing the spring composition, in addition to the soil CO_2 effect. The ratios for Maolan spring are more obscure due to lower evaporation by lower temperature and higher air humidity (Fig. 8).

pH

The relatively high alkalinity at the two sites means that the pH is regulated by the carbon dioxide levels in the water (Neal et al., 2002), i.e., as the partial pressure of carbon dioxide increases, pH decreases and vice versa. The pH changes observed in the springs thus mirror the P_{CO_2} changes but in an inverse way (Figures 2–7).

The decreased pH of spring water during summer storms could be also related to the lower pH of the rainfall (~7.2; Table 1), though the influence of rainfall may be small.

Calcite/dolomite saturation

As Neal et al. (2002) had shown that the temporal variation in the log SI simply mirrors the pH variability, reflecting both the biologically-induced seasonal and diurnal changes in dissolved carbon dioxide. At Nongla spring, the $SI_{calcite}$ and $SI_{dolomite}$ never fall below zero during November 1–3, 2003 (Fig. 4), and so no dissolution of limestone or dolomite is occurring here. However, in the epikarst aquifer, which feeds the spring, the $SI_{calcite}$ and $SI_{dolomite}$ may be below zero. Therefore, in the epikarst zone, it's the soil CO_2 effect caused by plant root respiration in soil that caused the diurnal hydrochemical change of the spring.

Further explanation of short-term storm-driven changes

Short-term storm-driven changes can be attributed to dilution or the shunting out of groundwater stored in the epikarst zone. This can be verified by some mass balance calculations:

$$Q_n \cdot c_n + Q_r \cdot c_r = Q_m \cdot c_m$$
$$\text{and} \quad Q_n + Q_r = Q_m$$

where Q = flow ($Q = 1.343 \times \text{stage}^{2.47}$ for Maolan, and $Q = 0.779 \times \text{stage}^{2.47}$ for Nongla), c = concentration of any particular species, m = spring flow showing the maximum storm effect, r = rainfall/groundwater input, and n = normal spring flow.

If Q is taken as fraction of maximum flow rather an absolute value, then $Q_n + Q_r = 1$. The ratio Q_m/Q_n = (stage m)$^{2.47}$/(stage n)$^{2.47}$; this can be used to calculate the fractions Q_n and Q_r.

Applying this to electrical conductivity (Spc, for c), the input water during the high intensity storm-event at Maolan spring (Fig. 7a) had an Spc of 235.75 and represented 98% of maximum flow; for the lower intensity storm at the same spring (Fig. 7b) the input water had an Spc of 340.26 and represented 94% of maximum flow (Table 4). Applying the calculation to P_{CO_2} shows that the P_{CO_2} of the input waters were 8293 and 6207 for both events. The results indicate that both storms shunted out moderately high conductivity groundwater. The contribution from direct overland flow during the higher intensity storm was greater, enough to dilute spring flow so that the Spc decreased during the maximum flow (but increased slightly soon afterwards). In contrast, during the low intensity storm, Spc increased because overland flow was a relatively minor proportion of maximum flow.

Applying the same calculations to the high and low intensity storms at Nongla spring (Figs. 6a and 6b), the input waters represented 93% and 94% of maximum flows respectively, and had Spcs of 152.43 and 237.25, about one fourth and half those of the base flows, P_{CO_2} of 2949 and 8037 respectively (Table 4). Thus the storms contributed a very large amount of overland flow to the spring. Therefore during the storms, the spring water was more dilute, reflecting the rainfall composition. Compared to Maolan spring, the hydrological conditions are clearly very different. This is be-

Table 4 Calculations of the base flow, maximum storm flow and relevant rainfall/groundwater input at both sites

Spr. Name	Time	Water stage (H, in m)	Q[a] (10^{-3} m^3/s)	Q_r (10^{-3} m^3/s)	Q_r/Q_m (%)	Spc (μs/cm)	Spc$_r$ (μs/cm)	P_{CO_2} (ppmv)	$P_{CO_{2r}}$ (ppmv)
Maolan	6:30, July 6, 2003	0.06	1.29	—	—	326.66	—	9419	—
	8:00, July 6, 2003	0.28	57.88	56.59	98	237.78	235.75	8318	8293
	3:45, July 19, 2004	0.06	1.29	—	—	317.91	—	5023	—
	7:00, July 19, 2004	0.19	22.21	20.92	94	338.96	340.26	6138	6207
Nongla	3:15, May 24, 2003	0.06	0.75	—	—	598.58	—	16,293	—
	5:30, May 24, 2003	0.18	11.27	10.52	93	182.12	152.43	3837	2949
	3:00, May 16, 2004	0.05	0.48	—	—	455.56	—	10,641	—
	5:45, May 16, 2004	0.16	8.43	7.95	94	249.68	237.25	8185	8037

[a] For Maolan spring, $Q = 1.343 \times H^{2.47}$, and $Q = 0.779 \times H^{2.47}$ for Nongla spring. (After the Ministry of Water Resources, PRC, 1991. Flow measurement by weirs and flumes. Industrial Standard, SL 24-91)

Table 5 Contribution of temperature, P_{CO_2} and lithology to concentrations of major ions in pure open carbonate—CO_2—H_2O system when approaching to equilibrium of carbonate dissolution[a]

T (°C)	P_{CO_2} (ppmv)	Lithology	Ca^{2+} (mg/l)	Mg^{2+} (mg/l)	HCO_3^- (mg/l)	pH
17.58	13,414	Limestone	81.20	0	247.05	7.19
		Dolomite	52.80	31.68	320.25	7.29
17.58	5439	Limestone	58.80	0	178.73	7.45
		Dolomite	38.40	23.04	231.80	7.56
16.53	13,414	Limestone	82.40	0	250.71	7.19
		Dolomite	54.00	32.40	327.57	7.30
16.53	5439	Limestone	60.00	0	182.39	7.45
		Dolomite	39.00	23.40	236.68	7.56

Note: Although dolomite is more soluble than calcite, it dissolves more slowly due to kinetic effects. However, in Nongla site with dolomite dominance, the spring water was saturated with both calcite and dolomite. In Maolan site with limestone dominance, the spring water was saturated with calcite but undersaturated with dolomite. This means that to compare the two sites, the kinetic effect is less important than solubility effect.

[a] The equilibrium calculation was according to Dreybrodt (1988).

cause that Nongla spring catchment has more bare rock, steeper slopes, less epikarst porosity.

Comparison of hydrochemistry between the two sites

Difference in general hydrochemistry

It can be seen from Table 2 that the Nongla spring has higher specific conductivity than Maolan spring.

The higher specific conductivity is related to both the higher CO_2 production in soil driven by higher temperature (Atkin et al., 2000; Edwards, 1975; Howard and Howard, 1993; Schwendenmann et al., 2003) and the higher percentage of dolomite in the Nongla Experimental Site. The former has been evidenced by higher temperature and P_{CO_2} in the Nongla spring (Table 2), and the latter is evidenced by elevated Ca^{2+}, Mg^{2+} and HCO_3^- in solution because the solubility of dolomite under natural conditions is higher than that of calcite (Dreybrodt, 1988). Table 5 shows the contribution of temperature, P_{CO_2} and lithology to $[Ca^{2+}]$, $[Mg^{2+}]$ and $[HCO_3^-]$, and thus specific conductivity of pure open carbonate–CO_2–H_2O system when approaching to equilibrium of carbonate dissolution. It can be seen that the difference in temperature between two sites shows little contribution to the difference in the concentrations of major ions in the solutions. However, the differences in both P_{CO_2} and lithology show comparable contributions to the discrepancies of major ion concentrations in the solutions.

Difference in hydrochemical response to rainfall

As showed before, electrical conductivity generally decrease after rainfall, and show inverse variation with water stage. However, for Maolan spring, electrical conductivity increases after lower rainfall. We attribute this to the soil CO_2 effect as discussed before (Liu et al., 2004). The reason why there is a difference in hydrochemical response to rainfall between the Maolan experimental site and the Nongla experimental site is that the water to the Maolan spring is possibly mainly supplied by soil water with higher P_{CO_2} (Liu et al., 2004; Edwards, 1975; Howard and Howard, 1993; Schwendenmann et al., 2003) via karst fractures, while the water to Nongla spring is mainly provided by rainwater with low P_{CO_2} via karst conduit and/or overland flow. In this latter case, dilution effect (Holloway and Dahlgren, 2001; Ahearn et al., 2004; Liu et al., 2004) dominate the change in electrical conductivity.

In addition, pH generally decreases after rainfall, and shows inverse variation with water stage (Figs. 6b, 7a and 7b). However, in some cases, pH increases after rainfall (Fig. 6a). This was possibly related to the influence of carbonate mineral dissolution from dusts at the site due to local human activities including limestone quarrying and road construction in 2003 (Liu et al., 2004).

Comparison with spring sites elsewhere in the world

At the observation site of Yudong (Fish-cave) Underground Stream, which is located at Zhen'an County of Shanxi Province, in a climatically transitional zone between North and South China, and the Guilin Karst Experimental Site, which is situated in the south part of China, Liu and Zhao (2000) found similar seasonal hydrochemical variations, i.e., with soil CO_2 partial pressure changing remarkably during a year (maximum in the summer growing season, and minimum in cold winter), the $[Ca^{2+}]$, $[HCO_3^-]$ and P_{CO_2} in water show almost synchronous remarkable change. That means it is the soil CO_2 that drives the seasonal hydrochemical variations in karst areas.

At Davys Creek Station, south-eastern Australia, Drysdale et al. (2003) also found a diurnal variation in hydrochemistry of a tufa-depositing stream. However, in their case, the pH values increased, and conductivity decreased at daytime, while the pH values decreased, and conductivity increased at nighttime. This is just opposite to our monitoring results. The authors attributed this behavior to the influence of diurnal temperatures on the solubility of CO_2 in water. In our case, it is the CO_2 produced by root respiration in soil that dominated the diurnal hydrochemical variations of the epikarst springs. We think the difference comes from where and what the examined water is. If CO_2 degasses from the spring water to the atmosphere, it will cause the pH to rise and the Spc to fall, particularly if calcite precipitates from the water. However, this happens generally at the place where spring water travels some distance. The Australian case belongs to this kind. In our case, the sensors were located just at the spring mouth, i.e., before the CO_2 could degas from the water. Therefore, our data are mainly reflection of the soil and epikarst aquifer, but not between the spring and the atmosphere.

Conclusions

The two-year continuous results show that both the Nongla and the Maolan springs are dynamic and variable systems in terms of hydrochemistry. Marked seasonal, diurnal and storm-scale variations are observed for pH, conductivity, CO_2 partial pressures and calcite/dolomite saturation indexes of the springs. However, the variability of these hydrochemical features tends to be seasonal $\geqslant$ storm-scale $>$ diurnal. The seasonal and diurnal variations of these features tend to co-vary with temperature which influences the production of CO_2 in soils, and is the primary driving force for the variations. The storm-scale fluctuations occur during the spring-summer rainy days due to the storm events. Depending on the rainfall intensities and the features of karst development, however, there are differences in amplitudes and direction of the variations of these features. At very high rainfall intensity, the dilution effect dominates the variations, characterized by the decrease in both conductivity and calcite/dolomite saturation of the springs, while soil CO_2 effect determines the variations at lower rainfall intensity, characterized by the decrease in pH and calcite/dolomite saturation but increase in CO_2 partial pressure and conductivity. In conclusion, the hydrobiogeochemical processes at the both sites are highly dynamic at the seasonal, diurnal and storm-event temporal scales and spatially complex at the watershed scale making management of epikarst spring hydrochemical compositions, such as pH and pH-sensitive element concentrations, very challenging.

Results from the study demonstrate the need to redesign hydrogeochemical sampling strategies for epikarst springs in karst areas with monsoon climate like SW China (i.e., with remarkable seasonal matching fluctuations in temperature, rainfall and vegetation), and also show that a continuous monitoring is necessary to get high accurate estimation of karst-related carbon flux (Liu and Zhao, 2000). Although the accurate estimation of karst-related carbon flux is not possible at the moment due to the problems in long-term spring water stage recording. However, large seasonal and storm-event variation (>3-fold) in dissolved inorganic carbon (evidenced by conductivity change) was found in epikarst systems by this study. So, the conventional stochastic sampling strategy may have an error of a factor of 3. In conclusion, to obtain karst-related carbon flux more accurately, it is necessary to conduct continuous hydrological and hydrochemical monitoring with sound sensors and data-loggers.

Acknowledgements

This work was supported by the National Natural Science Foundation of China (Grant No. 40572017), Chinese Academy of Science (CAS Program of 100 Distinguished Young Scientists), and Ministry of Science and Technology of China (Grant No. 2005DIB3J067). Special thanks are given to the two anonymous reviewers and editor for their valuable comments and suggestions, which improved the manuscript a lot.

References

Ahearn, D.S., Sheibley, R.W., Dahlgren, R.A., Keller, K.E., 2004. Temporal dynamics of stream water chemistry in the last free-flowing river draining the western Sierra Nevada, California. Journal of Hydrology 295, 47–63.

Andreo, B., Carrasco, F., Bakalowicz, M., Mudry, J., Vadillo, I., 2002. Use of hydrodynamic and hydrochemistry to characterise carbonate aquifers. Case study of the Blanca–Mijas unit (Malaga, southern Spain). Environmental Geology 43, 108–119.

Atkin, O.K., Edwards, E.J., Loverys, B.R., 2000. Response of root respiration to changes in temperature and its relevance to global warming. New Phytologist 147, 141–154.

Atkinson, T.C., 1977. Diffuse flow and conduit flow in limestone terrain in the Mendip Hills, Somerset (Great Britian). Journal of Hydrology 35, 93–110.

Drever, J.I., 1988. The Geochemistry of Natural Waters, second ed. Prentice-Hall, Englewood Cliffs.

Dreybrodt, W., 1988. Processes in karst systemsSpringer Series in Physical Environment. Springer, Heidelberg.

Drysdale, R., Lucas, S., Carthew, K., 2003. The influence of diurnal temperatures on the hydrochemistry of a tufa-depositing stream. Hydrological Processes 17, 3421–3441.

Edwards, N.T., 1975. Effects of temperature and moisture on carbon dioxide evolution in a mixed deciduous forest floor. Soil Science Society of America Proceedings 39, 361–365.

Farmer, J.J., Williams, S.D., 2001. Seasonal and short-term variability in chlorinated solvent concentrations in two karst springs in Middle Tennessee: Implications for sampling design. In: Kuniansky, E.L., (Ed.), U.S. Geological Survey Karst Interest Group Proceedings. Water-Resources Investigations Report 01-4011, pp. 141–149.

Field, M.S., 2002. A lexicon of cave and karst terminology with special reference to environmental karst hydrology, EPA/600/R-02/003.

Guasch, H., Armengol, J., Martí, E., Sabater, S., 1998. Diurnal variation in dissolved oxygen and carbon dioxide in two low-order streams. Water Research 32, 1067–1074.

Hess, J.W., White, W.B., 1988. Storm response of the karsitc carbonate aquifer of south central Kentuck. Journal of Hydrology 99, 235–252.

Holloway, J.M., Dahlgren, R.A., 2001. Seasonal and event-scale variations in solute chemistry for four Sierra Nevada catchments. Journal of Hydrology 250, 106–121.

Howard, D.M., Howard, P.J.A., 1993. Relationships between CO_2 evolution, moisture content and temperature for a range of soil types. Soil Biology and Biochemistry 25, 1537–1546.

Liu, Z., Zhao, J., 2000. Contribution of carbonate rock weathering to the atmospheric CO_2 sink. Environmental Geology 39, 1053–1058.

Liu, Z., He, S., Yuan, D., Zhao, J., 1998. Soil CO_2 and its drive to karst processes. Hydrogeology and Engineering Geology 25, 42–45 (In Chinese).

Liu, Z., Groves, C., Yuan, D., Meiman, J., Jiang, G., He, S., 2004. Hydrochemical variations during flood pulses in the southwest China peak cluster karst: Impacts of $CaCO_3$–H_2O–CO_2 interactions. Hydrological Processes 18, 2423–2437.

Liu, Z., Li, Q., Sun, H., Liao, C., Li, H., Wang, J., Wu, K., 2006. Diurnal variations of hydrochemistry in a travertine-depositing stream at Baishuitai, Yunnan, SW China. Aquatic Geochemistry 12, 103–121.

Maberly, S.C., 1996. Diel, episodic and seasonal changes in pH and concentrations of inorganic carbon in a productive lake. Freshwater Biology 35, 579–598.

Neal, C., Watts, C., Williams, R.J., Neal, M., Hill, L., Wickham, H., 2002. Diurnal and longer term patterns in carbon dioxide and calcite saturation for the River Kennet, south-eastern England. The Science of the Total Environment 282–283, 205–231.

Quinlan, J.F., Alexander Jr., E.C., 1987. How often should samples be taken at relevant locations for reliable monitoring of pollutants from an agricultural, waste disposal, or spill site in a karst terrane? A first approximation. In: Beck, B.F., Wilson, W.L. (Eds.), Proceedingsof Multidisciplinary Conference on Sinkholes and Environmental Impacts of Karst. A.A. Balkema, Rotterdam, pp. 277–293.

Quinlan, J.F., Ewers, R.O., 1985. Ground water flow in limestone terranes: Strategy rationale and procedure for reliable, efficient monitoring of ground water quality in karst areas. In: Proceedings of Fifth National symposium and exposition on aquifer restoration and ground water monitoring. National Water Well Association, Worthington, OH, pp. 197–234.

Raeisi, E., Karami, G., 1997. Hydrochemographs of Berghan karst spring as indicators of aquifer characteristics. Journal of Cave and Karst Studies 59, 112–118.

Ryan, M., Meiman, J., 1996. An examination of short-term variations in water quality at a karst spring in Kentucky. Ground Water 34, 23–30.

Schwendenmann, L., Veldkamp, E., Brenes, T., O'Brien, J.J., Mackensen, J., 2003. Spatial and temporal variation in soil CO_2 efflux in an old-growth neotropical rain forest, La Selva, Costa Rica. Biogeochemistry 64, 111–128.

Shuster, E.T., White, W.B., 1971. Seasonal fluctuations in the chemistry of limestone springs: A possible means for characterizing carbonate aquifers. Journal of Hydrology 14, 93–128.

Stumm, W., Morgan, J.J., 1981. Aquatic Chemistry, second ed. Wiley-Interscience, New York.

Suarez, DL., 1983. Calcite supersaturation and precipitation kinetics in the lower Colorado River. All American.Canal and East Highland Canal. Water Resources Research 19, 653–661.

Wigley, T.M.L., 1977. WATSPEC: a computer program for determining equilibrium speciation of aqueous solutions.

British Geomorphological Research Group Technical Bulletin 20, 1—48.

Zhang, C., Yuan, D., Cao, J., 2005. Analysis of the environmental sensitivities of a typical dynamic epikarst system at the Nongla monitoring site, Guangxi, China. Environmental Geology 47, 615—619.

Zhou, Z., 1987. Scientific Survey of the Maolan Karst Forest. Guizhou Peoples' Publishing House, Guiyang.